THE JOURNAL OF PHYSICAL CHEMISTRY B

Article

pubs.acs.org/JPCB

Effect of Single-Base Mutation on Activity and Folding of 10-23 Deoxyribozyme Studied by Three-Color Single-Molecule ALEX FRET

Jiwon Jung,[†] Kyu Young Han,[†] Hye Ran Koh,[†] Jihyun Lee,[†] Yoon Mi Choi,[†] Christine Kim,[‡] and Seong Keun Kim*[,†,§]

[†]Department of Chemistry, Seoul National University, Seoul 151-747, Korea

[‡]Columbia University Medical Center, New York, New York 10032, United States

[§]WCU Department of Biophysics and Chemical Biology, Seoul National University, Seoul 151-747, Korea

Supporting Information

ABSTRACT: We investigated the effect of single-base mutation on the RNA-cleaving activity and ion-induced folding of 10-23 deoxyribozyme at the single-molecule level by 3-color ALEX FRET (alternating laser excitation fluorescence resonance energy transfer). We found that substitution or deletion of a single base in the active region of the enzyme leads to a different folding pathway and enzymatic activity for all three mutants studied, but the severity of the effect was dependent on the type of mutation and the mutation site. We suggest that mutation of even a single base may result in a considerably different ionic and hydrogen-bonding interactions. Structural changes of 10-23 deoxyribozyme as it successively binds with Mg^{2+} and the substrate were also unambiguously identified by the current single-molecule-detection method.

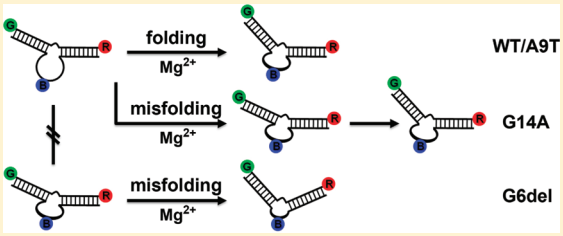

INTRODUCTION

Deoxyribozyme is a DNA molecule that possesses catalytic activities just as RNA or protein does.[1−4] Since its first inception by in vitro selection more than 10 years ago,[5,6] various forms of deoxyribozyme with diverse functions have been introduced. Deoxyribozyme may prove to be an ideal enzyme because of the much superior stability of DNA over RNA or protein in physiological conditions and the cost effectiveness of its synthesis.[6−12] Wide-ranging applications of deoxyribozymes are found in metal biosensors,[7,8] RNA biochemistry,[6,9] DNA computation,[10] and in vivo therapeutics,[11,12] In contrast to ribozymes for which extensive studies have been carried out on structure, catalysis, and folding,[13,14] only limited information is available about deoxyribozymes so far.[15−20]

Although some attention has lately been paid to the ion-induced folding of the RNA-cleaving 8-17 deoxyribozyme,[21−24] less is known about 10-23 deoxyribozyme, which is another well-known structural motif for RNA-cleaving activity.[25] In our own recent study on 8-17 deoxyribozyme using our newly developed 3-color ALEX FRET technique, we found a strong correlation between a key structure in the core region of 8-17 deoxyribozyme and its enzymatic activity.[23] In the present study, we turn our attention to lesser-known 10-23 deoxyribozyme, and by introducing single-base mutation this time, we found that even a minor degree of mutation at the catalytic site greatly affects its folding and enzymatic activity. It appears that the structure−function relationship for deoxyribozymes is acutely dependent on the conservation of a local structure. We also demonstrate the superior power of the single-molecule method over the previous ensemble measurements by showing that the structure of 10-23 deoxyribozyme undergoes distinctly identifiable steps of change as Mg^{2+} and the substrate are successively added.

EXPERIMENTAL METHODS

Sample Preparation. For structural examination of 10-23 deoxyribozyme itself (free from bound RNA substrate), we purchased from Integrated DNA Technologies (Coralville, IA) an HPLC-purified sample of 10-23 deoxyribozyme doubly labeled at its ends, with TAMRA at the 3′ end and Alexa647 at the 5′ end via an amino modifier C6 (Figure 1A). For the folding study of the enzyme−substrate complex, we prepared a doubly labeled noncleavable "deoxyribo-only" substrate and an enzyme labeled at its T8 position on the bulge with Alexa488 through the amino modifier C6 (Figure 1B), which is known to little affect the enzyme activity. For enzyme kinetic study of the RNA cleavage reaction, we used another substrate with the same sequence except for the two bases at the cleavage site (Figure 1A, red circle; deoxyuridine and deoxyadenine) replaced by uracil and adenine so that the substrate can now be readily cleaved by the enzyme. Finally, for our single-base mutation study, we adopted the following three mutants for comparison with the wild type ("WT"): "A9T" with the A at the position 9 substituted with a T; "G6del" whose G at the position 6 was deleted; and "G14A" with the G at the position

Received: December 6, 2011
Revised: February 7, 2012
Published: February 13, 2012

   dx.doi.org/10.1021/jp2117196 | J. Phys. Chem. B 2012, 116, 3007−3012

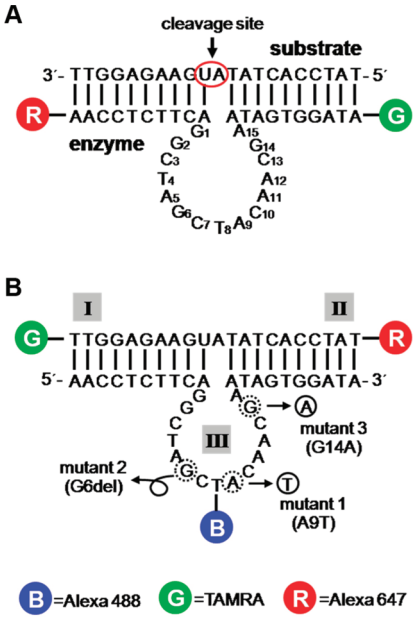

Figure 1. Secondary structure of (A) doubly and (B) triply labeled 10-23 deoxyribozyme−substrate complex. Uracil and adenine at the cleavage site indicated by arrow and red circle are RNA bases in the activity experiment. In the folding experiment, they are substituted by deoxyuridine and deoxyadenine to avoid substrate cleavage.

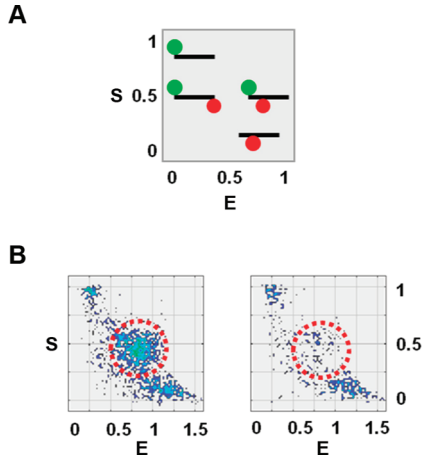

Figure 2. (A) Two-dimensional FRET efficiency (E)−stoichiometry (S) diagram representing green-only species (top left), green-red species with low E (middle left), green-red species with high E (middle right), and red-only species (bottom right). (B) Two-dimensional E−S diagrams for 10-23 deoxyribozyme activity experiment at 100 mM Mg^{2+} after an incubation time of 0 min (left) and 30 min (right). The doubly labeled substrate (represented by red dotted circle) is seen to disappear upon sufficient incubation with the enzyme, as a result of its cleavage reaction.

14 of the bulge substituted with an A (Figure 1B). The Alexa647 and Alexa488 dyes were purchased from Molecular Probes (Eugene, OR).

In order to remove impurities after attaching the dye to the modifier, we further purified our sample by 18 or 20% polyacrylamide/5 M urea gel, depending on the length of the oligomer. The enzyme and substrate were hybridized to form a double-stranded DNA complex by heating the sample in a solution of 25 mM Tris-HCl pH 8.0 and 500 mM NaCl for 2 min at 95 °C and cooling it to room temperature for more than 4 h. For our folding and kinetic experiments at the single-molecule level, we diluted our sample to ~50 pM concentration with the single-molecule buffer (50 mM Tris-HCl pH 7.0, 250 mM NaCl, 100 μg/mL BSA, 1 mM mercaptoethylamine, 5% glycerol).[23]

Ensemble Experiment. We used a spectrofluorometer (QM-4/2004SE, PTI, Lawrenceville, NJ) to measure the relative quantum yield of the dyes used in labeling 10-23 deoxyribozyme and its mutants in the ensemble level at various Mg^{2+} ion concentrations. We measured the emission from three dsDNAs (30 nM) at the magic angle polarization (54.7°), each singly labeled with one of the three dyes, at the Mg^{2+} concentrations of 0, 2.5, 25, and 100 mM. We found that the fluorescence intensity was not affected by Mg^{2+} concentration and stayed at a constant level with little variation. We also measured the fluorescence anisotropy value of each dye, which was 0.06 for Alexa488, 0.20 for TAMRA, and 0.23 for Alexa647 in the absence of Mg^{2+}. No significant changes were found upon increasing the Mg^{2+} concentration.

Single-Molecule-Detection Method. The ALEX FRET technique is a single-molecule-detection method based on multicolor FRET.[29,30] It allows simultaneous measurement of interprobe distance and selective observation of the species of our interest (Figure 2A) from a sample of heterogeneous mixture.[23,26−28] In our newly developed 3-color ALEX FRET detection, each molecule passes through the confocal volume in 1 ms diffusion time and is irradiated by a pulse train of three lasers in sequence that are alternately on for 36 μs with a 4 μs pause in between, and the resulting emissions from three dyes are respectively detected by three avalanche photodiodes. The blue dye B was excited by an Ar^{+} laser (35-LAP-321, Melles Griot, Carlsbad, CA) at 477 nm, the green dye G by a diode laser (TECGL-20, World Star Tech, Toronto, Canada) at 532 nm, and the red dye R by a HeNe laser (25-LHP-925, Melles Griot, Carlsbad, CA) at 633 nm. The laser power we used was 60 μW at 477 and 532 nm and 24 μW at 633 nm. Any signal due to imperfectly labeled species inadvertently introduced during sample preparation can be discarded by the 3-color ALEX technique that selectively detects only the triply labeled species by rejecting the signals from singly and doubly labeled impurities. Using our data analysis method,[28] we obtained a set of three interprobe FRET efficiency values (E) at different Mg^{2+} concentrations, and then applied the following equations to calculate the apparent dissociation constant K_d:[13]

$$E = E_i + \Delta E[Mg^{2+}]/([Mg^{2+}] + K_d) \quad (1)$$

$$E = E_i + \Delta E_1[Mg^{2+}]/([Mg^{2+}] + K_{d1}) + \Delta E_2[Mg^{2+}]/([Mg^{2+}] + K_{d2}) \quad (2)$$

Here, E_i is the E value in the initial unfolded state and ΔE is the change in the E value upon addition of Mg^{2+}. Equation 2 can be applied to a two-step folding process. All E values measured for each interprobe dye pair and the corresponding K_d values are listed in Table 1. With our data analysis method, we also can obtain the stoichiometry values (S) at different Mg^{2+} concentrations using the following equation

$$S = F_{Dexc}/(F_{Dexc} + F_{Aexc}) \quad (3)$$

where F_{Dexc} and F_{Aexc} represent the total photon counts when the excitation is performed with the donor-exciting laser and the acceptor-exciting laser, respectively.

dx.doi.org/10.1021/jp2117196 | J. Phys. Chem. B 2012, 116, 3007−3012

Table 1. Values of E_i, ΔE, E_f (=E_i + ΔE), and K_d for WT 10-23 Deoxyribozyme and Its Three Mutants[a]

	GR				BR				BG			
	E_i	ΔE	E_f	K_d	E_i	ΔE	E_f	K_d	E_i	ΔE	E_f	K_d
WT	0.42	0.06	0.48	9.9	0.41	0.09	0.50	7.8	0.26	0.06	0.32	5.5
A9T	0.42	0.09	0.51	7.5	0.44	0.12	0.56	7.5	0.27	0.07	0.34	7.8
G6del	0.45	0.14	0.59	6.8	0.47	0.14	0.61	3.2	0.35	NA	NA	NA
G14A	0.46	0.07	0.53	10.1	0.39	0.06, 0.12	0.55	0.57, 10.1	0.29	0.07	0.36	0.83

[a]Entries with two values represent two-step folding.

RESULTS AND DISCUSSION

Activity Test for Dye-Labeled Wild-Type 10-23 Deoxyribozyme and Its Mutants. Since our FRET experiments require dye-labeling of enzymes that may affect their activity, we compared the enzyme activity of the WT 10-23 deoxyribozyme in its unlabeled versus labeled form to verify that dye-labeling does not seriously affect the enzyme activity. When we incubated the mixture of enzyme and substrate in SM buffer at 100 mM Mg^{2+} and 37 °C for 30 min, the dye-labeled enzyme showed a strong substrate-cleaving activity as seen from the large decrease in signal at $S \sim 0.5$ (Figure 2B, red dotted circles). In order to compare the cleavage rate of the unlabeled versus labeled enzymes, we varied the incubation time of the sample at 100 mM Mg^{2+}, and found that the cleavage rate of the enzyme was not critically affected by labeling (Figure 3, black versus red curves). The measured decay time was 45.4 ± 4.3 and 62.5 ± 11.4 min for the unlabeled and labeled WT 10-23 deoxyribozyme, respectively.

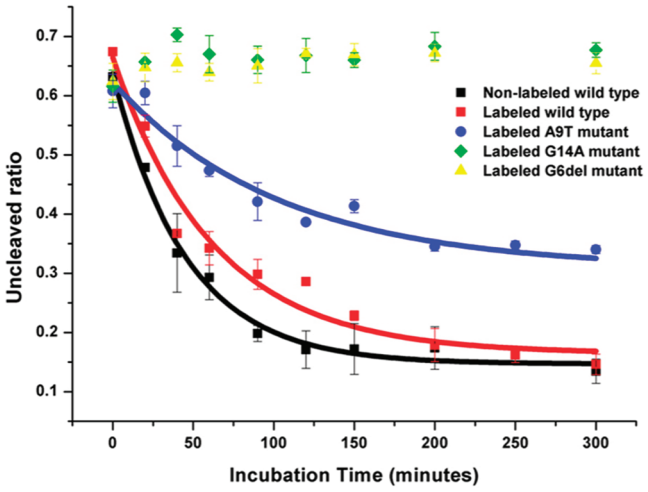

Figure 3. Ratio of uncleaved substrate against incubation time for unlabeled (black) and labeled (red) WT 10-23 deoxyribozyme and three labeled mutants, A9T (blue), G14A (green), and G6del (yellow) at 100 mM [Mg^{2+}] and room temperature (22 °C). All curves are fitted with the first-order exponential function.

Enzyme Activity of Single Base-Mutated 10-23 Deoxyribozymes. We also measured the enzyme activity of the three mutants of 10-23 deoxyribozyme using 3-color ALEX. Figure 3 shows that the substrate-cleaving activity of A9T is quite considerably conserved (blue curve), with a decay time of 103.0 ± 18.5 min, whereas G6del and G14A lose their activity altogether (yellow and green dots, respectively). Similar results were obtained by conventional gel analysis at the ensemble level,[18,20] but we note that the current study provides unequivocal demonstration for the drastic effect of single-base mutation at the single molecule level. All decay curves of Figure 3 were fitted by a first-order exponential function.

Binding of Mg^{2+} with 10-23 Deoxyribozyme for Activity and Folding. Metal ions not only govern the overall dielectric property of the enzyme solution but also affect the local structure of the enzyme and the solvation structure around it. Assuming that the RNA-cleaving activity of the enzyme is somehow closely related to its folding structure through the typical structure−function relationship, we expect the dissociation constant (K_d) of the metal ion (typically Mg^{2+}) in the activity measurement to be closely related to that in the folding study.

We carried out the measurement of K_d by varying the concentration of Mg^{2+} from 0 to 75 mM while allowing its incubation with WT 10-23 deoxyribozyme for different incubation times of 40, 120, and 200 min at 22 °C. The noncooperative binding model predicts the following hyperbolic function for dissociation,[16] to which our result was fitted well (Figure S1 in the Supporting Information):

$$V = \frac{V_{max}[Mg^{2+}]}{K_d + [Mg^{2+}]} \quad (4)$$

We obtained dissociation constants of 9.2 ± 0.9, 9.6 ± 0.9, and 6.8 ± 0.8 mM for the incubation times of 40, 120, and 200 min, respectively. As we expected above, these values of K_d obtained from the activity test of WT 10-23 deoxyribozyme are in reasonable agreement with the K_d values from our folding study of WT 10-23 deoxyribozyme and A9T, the activity-conserving mutant, but not with the K_d values of G14A and G6del, the two other mutants with no activity (Table 1).

Structural Transitions of 10-23 Deoxyribozyme with Mg^{2+} and Substrate. 10-23 deoxyribozyme consists of two stems (labeled I and II in Figure 1B) and a 15-residue catalytic core that forms a bulge (labeled III), which respectively recognize the substrate and cleaves its specific RNA site upon adding a cofactor such as Mg^{2+}.[6,18−20] Before embarking on the folding experiment, we first investigated how the structure of 10-23 deoxyribozyme itself changes as a function of [Mg^{2+}] in the absence of substrate by applying the 2-color ALEX FRET technique to a 10-23 deoxyribozyme sample labeled with a green and red fluorophore at either end of the stems (Figure 1A).

A single-stranded DNA usually exists in the form of a random coil but changes to a more compact structure upon adding a metal cation that often compensates the negative charge on the phosphate backbone of DNA.[31,32] Interestingly, in a previous FRET study for the structural transition of 10-23 deoxyribozyme that was conducted at the ensemble level, the enzyme strand was found to undergo a transition from an extended structure to something similar to the enzyme−substrate complex with a trace amount of Mg^{2+},[25] which could

dx.doi.org/10.1021/jp2117196 | J. Phys. Chem. B 2012, 116, 3007−3012

be misinterpreted as if the enzyme obtains its ultimate structure by Mg^{2+} alone even before it binds to the substrate.

First of all, we find in the current single-molecule study that 10-23 deoxyribozyme obtains a distinctly more compact structure (characterized by the increase of the E value from 0.80 to 0.93 in the last two diagrams in the bottom panel of Figure 4) when Mg^{2+} is added. Next, with the addition of the substrate, the structure now becomes much more extended (E = 0.55, the third diagram in the bottom panel of Figure 4). In all these diagrams, the stoichiometric parameter (S) value of 0.5 indicates that our sample is fully labeled with the green and red dyes. Since a DNA with a long bulge often fails to attain complete hybridization with the substrate because of the random dynamic motion of the latter,[33] it is possible that the previous ensemble result could have been affected by the general difficulty of making an accurate FRET measurement in an ensemble of heterogeneous mixture with different degrees of hybridization.

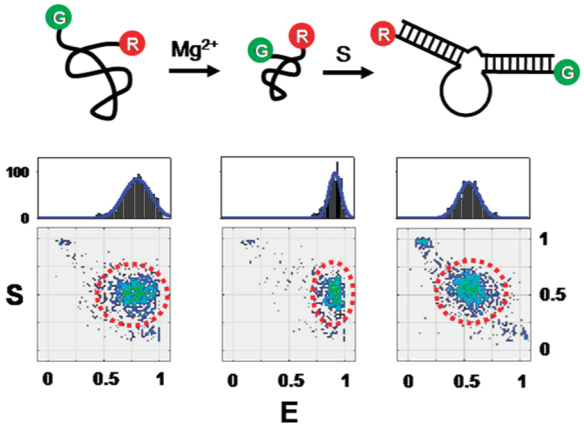

Figure 4. Two-dimensional E–S diagrams and the corresponding schematic structures of 10-23 deoxyribozyme, with no Mg^{2+} or substrate (left), with only Mg^{2+} at 25 mM (center), and with both Mg^{2+} (25 mM) and substrate (right). Above each E–S diagram, a one-dimensional E histogram is shown (gray) with a Gaussian fitting curve (blue).

Global Folding of the Wild-Type 10-23 Deoxyribozyme. The most vital issue in the global folding of multibranched nucleotides such as 10-23 deoxyribozyme is to find out how intimately the substrate-binding arms and the highly flexible bulge work together to effect catalytic activity. For the triply labeled complex (Figure 1B), we employed the 3c-ALEX FRET technique to simultaneously detect the motion of all three branches of the WT 10-23 deoxyribozyme by tracking its Gaussian-fitted average E values as we increased [Mg^{2+}] from 0 to 100 mM. The result, repetitively represented by squares connected by the blue curve in each panel of Figure 5, shows a gradual decrease in all three interprobe distances, indicated by the corresponding increase in E: 0.42 → 0.48 between stem I and II (GR), 0.41 → 0.50 between stem II and bulge (BR), and 0.26 → 0.32 between stem I and bulge (BG). The apparent dissociation constant (K_d) for each pair of probes calculated by eqs 1 and 2 is 9.9 ± 1.9, 5.5 ± 0.9, and 7.8 ± 1.0 mM, respectively, which suggest that, as mentioned in the kinetic part, the activity and the folding process are closely related and also that WT 10-23 deoxyribozyme undergoes global folding into a triangular pyramidal shape as in does 8-17 deoxyribozyme.[21−23]

Folding of the 10-23 Deoxyribozyme Mutants. In order to see if there exists more direct correlation between folding and activity, we chose the following three mutants for comparison: A9T with A at the position 9 substituted by T; G6del whose G at the position 6 was deleted; and G14A with the G at the position 14 of the bulge substituted by A (Figure 1, A and B). The last two are known to have a drastically lowered cleavage rate than WT, whereas the first mutant retains much of its activity.[18,20] The folding data for A9T in the left column of panels of Figure 5 (represented by circles connected by red

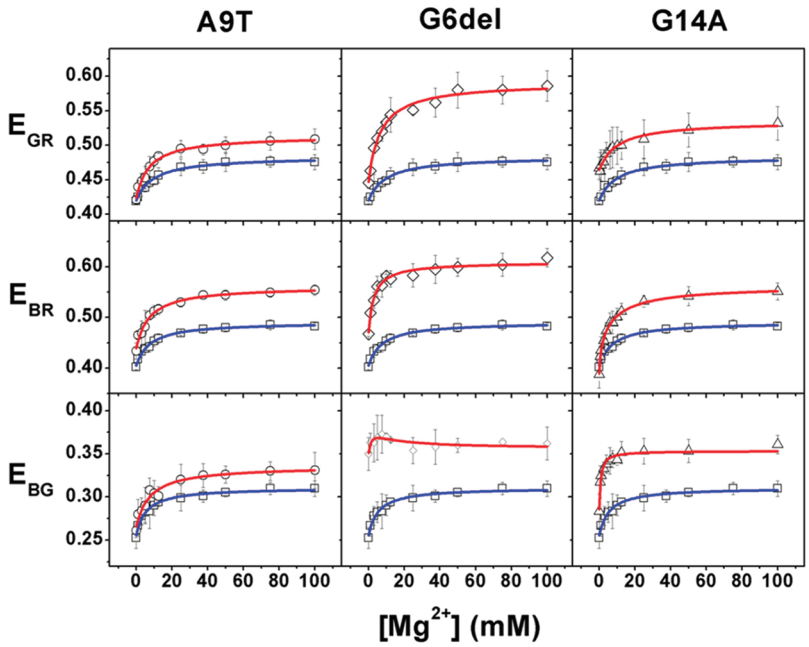

Figure 5. [Mg^{2+}]-dependent changes in the three E values of WT 10-23 deoxyribozyme (blue) and its three mutants (red). The blue curves are shown repetitively in each row of panels for expedient comparison with red curves.

dx.doi.org/10.1021/jp2117196 | J. Phys. Chem. B 2012, 116, 3007–3012

lines) indicate a rather similar overall behavior to that of WT, with only a small difference in the initial and final structure. We can therefore infer that the position 9 that is little affected by substitution is not directly involved in forming the catalytic center of 10-23 deoxyribozyme. A recent phosphorothioate modification study suggests that the nonbridging phosphate oxygen atoms in 10-23 deoxyribozyme from P9 to P13 coordinate directly to divalent ions.[34] Therefore, the A9T mutation that hardly affects the structure of phosphate backbone should have little influence on the global folding and the enzymatic activity.

In contrast, the initial and final structures of mutant G6del in the middle column of panels of Figure 5 (diamonds connected by red lines) are considerably different from those of WT, in particular with regard to BG that represents the folding between stem I and the bulge. Based on nucleotide analogue substitution experiments, it was suggested that divalent metal ions coordinate to the carbonyl oxygen of G6 and the nearby nonbridging phosphate to make them the active catalytic core of 10-23 deoxyribozyme.[18,34] A large change in the overall structure of G6del such as represented by Figure 5 should prevent proper folding of the catalytic region.

On the other hand, for the third mutant G14A, the folding behavior shown in the right column of panels of Figure 5 (triangles connected by red lines) is seemingly not as clearly different from that of WT, except that the folding of BG occurs at very low [Mg^{2+}], with a K_d value of 0.8 ± 0.2 mM. Such a distinct two-step folding behavior was also observed in the folding of hammerhead ribozyme[13] and the Zn^{2+}-dependent folding of 8-17 deoxyribozyme.[21] Unlike these other cases that involve substrate folding in their first step, however, the folding of the mutant G14A starts with misfolding of the catalytic region, which ultimately leads to its failure to obtain a proper structure for cleavage reaction. Examples of such misfolding or arrested folding can be found in some mutants of hammerhead ribozyme.[35]

The current comparative study provides direct evidence at the single-molecule level that there indeed exists a strong correlation between enzymatic activity and the folding of 10-23 deoxyribozyme that goes beyond random variation in activity resulting from a simple sequence change. Overall, 10-23 deoxyribozyme shows similar folding features to those of 8-17 deoxyribozyme, including a relatively small degree of conformational change and the transition to a more compact structure.

A succinct summary comparing the different folding behaviors of 10-23 deoxyribozyme and its mutants is schematically given in Figure 6. According to an earlier study for 8-17 deoxyribozyme by single-molecule FRET (smFRET),[24] no dynamic equilibrium between its folded and unfolded states was observed, which suggests that the biophysics of a deoxyribozyme may be quite different from that of a ribozyme, although we cannot rule out the possibility that the time scale of the deoxyribozyme folding is so fast that smFRET cannot fully track the reaction pathway. One may consider studying the faster dynamics of 10-23 deoxyribozyme by fluorescence correlation spectroscopy,[36] but it may turn out to be quite difficult because of the small distance change associated with its folding.

CONCLUSIONS

We found that single-base mutations in nucleotide sequence of 10-23 deoxyribozyme by substitution or deletion lead to distinctly different folding pathways with correspondingly different enzymatic activity. The current work may be readily extended to elucidate the photophysical properties of transient single-stranded DNA that exists abundantly in living organisms.[37]

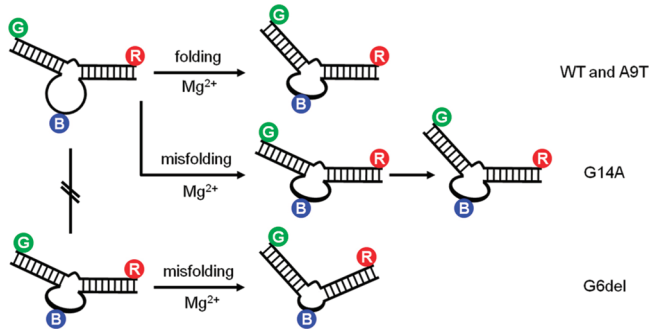

Figure 6. A schematic diagram for the different folding pathways of 10-23 deoxyribozyme and its mutants. The initial and final structures of WT, A9T, and G14A are generically similar, but those of G6del are substantially different. G14A exhibits a distinct two-step folding behavior.

ASSOCIATED CONTENT

Supporting Information

Figure showing ratio of cleaved substrate against [Mg^{2+}] after different incubation times. This material is available free of charge via the Internet at http://pubs.acs.org.

AUTHOR INFORMATION

Corresponding Author

*E-mail: seongkim@snu.ac.kr.

Notes

The authors declare no competing financial interest.

ACKNOWLEDGMENTS

This work was supported by the Chemical Genomics Grant (M10526020002-08N2602-00210), the Star Faculty Program (KRF-2005-084-C00017), the Global Frontier R&D Program on Center for Multiscale Energy System, and the World Class University Program (R31-2010-100320) of the National Research Foundation of Korea.

REFERENCES

(1) Breaker, R. R. *Nat. Biotechnol.* **1997**, *15*, 427−431.
(2) Peracchi, A. *ChemBioChem* **2005**, *6*, 1316−1322.
(3) Silverman, S. K. *Nucleic Acids Res.* **2005**, *33*, 6151−6163.
(4) Hobartner, C.; Silverman, S. K. *Biopolymer* **2007**, *87*, 279−292.
(5) Breaker, R. R.; Joyce, G. F. *Chem. Biol.* **1994**, *1*, 223−229.
(6) Santoro, S. W.; Joyce, G. F. *Proc. Natl. Acad. Sci. U.S.A.* **1997**, *94*, 4262−4266.
(7) Li, J.; Lu, Y. *J. Am. Chem. Soc.* **2000**, *122*, 10466−10467.
(8) Liu, J. W.; Lu, Y. *J. Am. Chem. Soc.* **2003**, *125*, 6642−6643.
(9) Purtha, W. E.; Coppins, R. L.; Smalley, M. K.; Silverman, S. K. *J. Am. Chem. Soc.* **2005**, *127*, 13124−13125.
(10) Stojanovic, M. N.; Stefanovic, D. *Nat. Biotechnol.* **2003**, *21*, 1069−1074.
(11) Sun, L. Q.; Cairns, M. J.; Saravolac, E. G.; Baker, A.; Gerlach, W. L. *Pharmacol. Rev.* **2000**, *52*, 325−347.
(12) Mitchell, A.; Dass, C. R.; Sun, L. Q.; Khachigian, L. M. *Nucleic Acids Res.* **2004**, *32*, 3065−3069.
(13) Bassi, G. S.; Murchie, A. I.; Walter, F.; Clegg, R. M.; Lilley, D. M. *EMBO J.* **1997**, *16*, 7481−7489.

(14) Zhuang, X. *Annu. Rev. Biophys. Biomol. Struct.* **2005**, *34*, 399−414.
(15) Santoro, S. W.; Joyce, G. F. *Biochemistry* **1998**, *37*, 13330−13342.
(16) Bonaccio, M.; Credali, A.; Peracchi, A. *Nucleic Acids Res.* **2004**, *32*, 916−925.
(17) Peracchi, A.; Bonaccio, M.; Clerici, M. *J. Mol. Biol.* **2005**, *352*, 783−794.
(18) Zaborowska, Z.; Furste, J. P.; Erdmann, V. A.; Kurreck, J. *J. Biol. Chem.* **2002**, *277*, 40617−40622.
(19) Schubert, S.; Gul, D. C.; Grunert, H. P.; Zeichhardt, H.; Erdmann, V. A.; Kurreck, J. *Nucleic Acids Res.* **2003**, *31*, 5982−5992.
(20) Zaborowska, Z.; Schubert, S.; Kurreck, J.; Erdmann, V. A. *FEBS Lett.* **2005**, *579*, 554−558.
(21) Liu, J.; Lu, Y. *J. Am. Chem. Soc.* **2002**, *124*, 15208−15216.
(22) Kim, H. K.; Liu, J.; Li, J.; Nagraj, N.; Li, M.; Pavot, C. M.; Lu, Y. *J. Am. Chem. Soc.* **2007**, *129*, 6896−6902.
(23) Lee, N. K.; Koh, H. R.; Han, K. Y.; Kim, S. K. *J. Am. Chem. Soc.* **2007**, *129*, 15526−15534.
(24) Kim, H.-K.; Rasnik, I.; Liu, J.; Ha, T.; Lu, Y. *Nat. Chem. Biol.* **2007**, *3*, 763−768.
(25) Cieslak, M.; Szymanski, J.; Adamiak, R. W.; Cierniewski, C. S. *J. Biol. Chem.* **2003**, *278*, 47987−47996.
(26) Kapanidis, A. N.; Lee, N. K.; Laurence, T. A.; Doose, S.; Margeat, E.; Weiss, S. *Proc. Natl. Acad. Sci. U.S.A.* **2004**, *101*, 8936−8941.
(27) Lee, N. K.; Kapanidis, A. N.; Wang, Y.; Michalet, X.; Mukhopadhyay, J.; Ebright, R. H.; Weiss, S. *Biophys. J.* **2005**, *88*, 2939−2953.
(28) Lee, N. K.; Kapanidis, A. N.; Koh, H. R.; Korlann, Y.; Ho, S. O.; Kim, Y.; Gassman, N.; Kim, S. K.; Weiss, S. *Biophys. J.* **2007**, *92*, 303−312.
(29) Lee, J. W.; Lee, S. H.; Ragunathan, K.; Joo, C. M.; Ha, T. J.; Hohng, S. C. *Angew. Chem., Int. Ed.* **2010**, *122*, 10118−10121.
(30) Stein, H. I.; Steinhauer, C.; Tinnefeld, P. *J. Am. Chem. Soc.* **2011**, *133*, 4193−4195.
(31) Mills, J. B.; Vacano, E.; Hagerman, P. J. *J. Mol. Biol.* **1999**, *285*, 245−257.
(32) Murphy, M. C.; Rasnik, I.; Cheng, W.; Lohman, T. M.; Ha, T. *Biophys. J.* **2004**, *86*, 2530−2537.
(33) Gohlke, C.; Murchie, A. I.; Lilley, D. M.; Clegg, R. M. *Proc. Natl. Acad. Sci. U.S.A.* **1994**, *91*, 11660−11664.
(34) Nawrot, B.; Widera, K.; Wojcik, M.; Rebowska, B.; Nowak, G.; Stec, W. J. *FEBS J.* **2007**, *274*, 1062−1072.
(35) Bassi, G. S.; Mollegaard, N. E.; Murchie, A. I.; Lilley, D. M. *Biochemistry* **1999**, *38*, 3345−3354.
(36) Li, H. T.; Ren, X. J.; Ying, L. M.; Balasubramanian, S.; Klenerman, D. *Proc. Natl. Acad. Sci. U.S.A.* **2004**, *101*, 14425−14430.
(37) Vilar, J. M.; Saiz, L. *Curr. Opin. Genet. Dev.* **2005**, *15*, 136−144.